ARTICLE
Journal of Cellular Biochemistry 108:169–180 (2009)

Journal of Cellular Biochemistry

NF-kappa B Is Required for the Development of Tumor Spheroids

J.C. Gallardo-Pérez,[1] M. Espinosa,[2] G. Ceballos-Cancino,[2] A. Daniel,[1] S. Rodríguez-Enríquez,[3] A. Aviles,[1] R. Moreno-Sánchez,[3] J. Melendez-Zajgla,[2**] and V. Maldonado[1*]

[1]*Molecular Biology Laboratory, Sub-Direction of Basic Research, National Institute of Cancerology, Mexico City, Mexico*

[2]*Functional Genomics Laboratory, National Institute of Genomic Medicine, Mexico City, Mexico*

[3]*Department of Biochemistry, National Institute of Cardiology ''Ignacio Chávez,'' Mexico City, Mexico*

ABSTRACT

Tumor cells cultured in three-dimensional models provide a more realistic and biologically meaningful analysis of the initial phases of cancer development and drug resistance. Several studies have demonstrated that culture of cancer cells in three dimensions induces cellular resistance to a variety of anti-neoplastic drugs by poorly understood mechanisms. The role of the transcription factor NF-κB and inhibitors of apoptosis proteins (IAPs) in the onset and development of drug resistance during tumor spheroid growth has not been established. In this work, we found a significant increase in the activity and expression of NF-κB and its downstream target XIAP (X-linked IAP) in cancer cells grown as multi-cellular tumor spheroids. Blocking XIAP expression with RNA interference markedly increased the sensitivity of cancer tumor spheroid cells toward anti-neoplastic drugs, indicating a role for IAPs in establishing drug resistance. In turn, inhibition of NF-κB by negative dominants suppressed spheroid formation, whereas overexpression of the upstream kinase IκBKβ increased their growth and resistance. The present data suggested that NF-κB and its downstream target XIAP were essential for the growth and drug resistance of small avascular tumor. J. Cell. Biochem. 108: 169–180, 2009.

KEY WORDS: CANCER; TRANSDUCTION PATHWAYS; DRUG RESISTANCE; NF-KAPPA B; THREE-DIMENSIONAL CELL CULTURE; X-LINKED INHIBITOR OF APOPTOSIS PROTEINS

Tumor cells may aggregate and interact in three dimensions to form multi-cellular tumor spheroids (MTS). This cellular array causes oxygen and nutrient gradients to develop between the inner and external layers, thus generating hypoxic and nutrient-deficient microenvironments [Sutherland, 1988]. Differences in gene expression among the spheroid cell layers [Shweiki et al., 1995] promote biochemical and physiological changes [Rodriguez-Enriquez et al., 2008], and behavior modifications of small avascular tumors in vivo [Kunz-Schughart, 1999]. Therefore, MTS constitute an excellent in vitro experimental model that mimics the complexity of a solid tumor [Mueller-Klieser, 1987].Since the cells in the external layers of an MTS are in contact with high concentrations of oxygen, nutrients, and growth factors, they are able to maintain a high proliferation index [Burkowski, 1977]. In contrast, cells in the central area are poorly provided with oxygen, nutrients, and growth factors, which induces the overexpression of pro-apoptotic proteins such as Bax, and hence apoptosis and necrosis [Khaitan et al., 2006]. Cells in the intermediate layers of the MTS are in a quiescent state regarding

Abbreviations used: MTS, multi-cellular tumor spheroid; XIAP, X-linked inhibitor of apoptosis protein; cIAP-1, cellular inhibitor of apoptosis-1; NF-κB, nuclear factor kappa B; IκBKβ, inhibitor of kappa B kinase beta; Bcl-3, B-cell lymphoma-3; HIF-1α, hypoxia-inducible factor-1α.

Grant sponsor: Consejo Nacional de Ciencia y Tecnologia (CONACyT); Grant number: CO1 42309.

*Correspondence to: V. Maldonado, Molecular Biology Laboratory, Sub-Direction of Basic Research, National Institute of Cancerology, Av. San Fernando 22, Tlalpan 14080, Mexico City, Mexico. E-mail: vilmaml@gmail.com

**Correspondence to: Dr. J. Melendez-Zajgla, Functional Genomics Laboratory, Research Direction, National Institute of Genomic Medicine, Periférico Sur No. 4124, Torre Zafiro II, Piso 6 Col. Ex Rancho de Anzaldo, Álvaro Obregón 01900, Mexico City, Mexico. E-mail: jmelendez@inmegen.gob.mx

Received 15 January 2009; Accepted 8 May 2009 • DOI 10.1002/jcb.22237 • © 2009 Wiley-Liss, Inc.

Published online 26 June 2009 in Wiley InterScience (www.interscience.wiley.com).

proliferation and intermediary metabolism [Freyer, 1998]; they also show a high tendency to differentiate [Kunz-Schughart, 1999].

Tumor spheroids from several sources show resistance to radiation [Dertinger and Hulser, 1981] and to high concentrations of several anti-neoplastic drugs [Olive and Durand, 1994]. It is well documented that in MTS, in contrast to monolayer models, several changes occur in the expression and sub-cellular distribution of proteins involved in tumor drug resistance such as P-glycoprotein [Xing et al., 2007], topoisomerase IIα [Oloumi et al., 2000], p21 [St Croix et al., 1996], MDR1 [Kolchinsky and Roninson, 1997], E-cadherins, and AKT pathway components [Kang et al., 2007]. However, the mechanisms involved in the acquisition of drug resistance have not been completely elucidated.

Most chemotherapeutic treatments induce cell death by releasing mitochondrial proteins to the cytosol, where they activate caspases that degrade key substrates, leading to apoptosis. Usually, cancer cells overexpress caspases 3, 7 or 9; in some cases, these proteins are also constitutively activated [Philchenkov, 2004]. Cancer cells survive caspase action by overexpressing inhibitory proteins such as X-linked inhibitor of apoptosis protein (XIAP), the most abundant member of the inhibitor of apoptosis protein (IAP) family [Nachmias et al., 2004]. An imbalance in the survival versus death pathways can favor cellular resistance to diverse hostile microenvironments and apoptotic stimuli, including anti-neoplastic drugs.

Nuclear factor kappa B (NF-κB) is the key member of the survival transduction pathway, and is commonly overexpressed or constitutively active in cancer cells such as human leukemia and colorectal and prostate cancers [Cilloni et al., 2006]. In unstimulated cells, NF-κB is located in the cytosol constitutively bound to inhibitory proteins of the IκB family, so that this factor is maintained in inactive dimeric complexes. After a stimulus, IκB is phosphorylated and degraded by the proteosome pathway. Proteosome degradation of IκB releases monomeric NF-κB and promotes its internalization by the nucleus, inducing the transcriptional transactivation of specific genes [Zhivotovsky and Orrenius, 2006]. NF-κB mediates the transcription of genes involved in the inflammatory and immune responses, the induction of cancer and the regulation of apoptosis [Okamoto et al., 2007]. It has also been implicated in carcinogenesis and in cellular resistance to chemotherapy [Piva et al., 2006]. Interestingly, NF-κB is activated by hypoxia, acidic pH, and nutrient deficiency, conditions usually found in the tumor microenvironment [Bonello et al., 2007].

Chemo-resistance of solid tumors has been found in response to drugs such as taxol (a mitotic inhibitor that causes cell death by disrupting the normal microtubule dynamics), cisplatin (a DNA damaging agent that induces apoptosis), staurosporine (a protein kinase inhibitor that affects survival pathways), and tamoxifen (an estrogen receptor modulator that blocks cell cycle). Furthermore, these drugs are commonly used in cancer treatment including cervical, breast, and head and neck carcinomas and chemo-resistance is observed in all cases [Mekhail and Markman, 2002]. In the present work, the mechanisms by which MTS acquire resistance toward cisplatin, taxol, tamoxifen, and staurosporine were analyzed. The four anti-neoplastic drugs were applied to MTS at doses similar to those used in the clinical practice. As these anti-neoplastic drugs have different targets, it was evaluated whether the resistance mechanisms were shared among them. It was found that MTS resistance to the four anti-neoplastic drugs was associated with increased XIAP levels, which in turn were connected to the activation of the NF-κB pathway and to the hypoxia generated in the inner and intermediate layers of the MTS.

MATERIALS AND METHODS

MTS CULTURE

Cancer cell lines 293 (a human transformed embryonic kidney cell line), T-47D (human breast cancer), HeLa (human cervical cancer), and KB (human head and neck cancer) were obtained from the ATCC and grown to sub-confluence as monolayers in DMEM (Gibco BRL, NY) supplemented with 8% fetal bovine serum (FBS) at 37°C in a humidified atmosphere of 5% (v/v) CO_2 in air. Spheroids were cultured by the liquid overlay technique as previously described [Yuhas et al., 1977]. Aliquots of 50,000 cells were cultured in 2% agarose on Petri dishes for 1 week and then placed in a rotary incubator at 37°C with Leibovitz L-15 medium (Invitrogen, CA) supplemented with FBS. The medium was changed every 2 days to avoid cytotoxicity. Spheroid diameters were measured at times indicated for each cell line using an eyepiece reticule (Zeiss, Germany). The volumes of at least 10 spheroids were calculated using the formula $V = 4/3\pi r^3$.

CELL VIABILITY ASSAYS

Cells grown as monolayers were seeded at 5×10^4 cells/well in 24-well plates and exposed for 24 or 48 h to staurosporine, taxol, or cisplatin (all at 0.1–400 μM), or tamoxifen (12.5–75 μM), to determine IC_{50} values (see Table I). After drug exposure, cell viability was determined by the crystal violet method [Baker et al., 1986]. Briefly, the cells were fixed in 70% ethanol for 10 min at −20°C, and then stained with 1% vital colorant in 70% ethanol for 20 min, washed several times and dissolved in 33% (v/v) acetic acid. Viability was determined from the absorbance changes at 570 nm. Means were calculated from at least three independent experiments performed in triplicate.

CELLULAR PASSAGE

From the four cell lines employed to generating spheroids, two were selected for "cellular passage experiments." Thus, to compare mechanisms of drug resistance, a human transformed (293) cell line that produce large spheroids in a few days and a human cancer cell line

TABLE I. IC_{50} Values Obtained in Monolayer Cells in the Presence of Anti-Neoplastic Drugs

	IC_{50} (μM)	
	T-47D	293
Taxol	0.3 ± 0.01	205 ± 0.05
Cisplatin	333 ± 0.6	198 ± 0.13
Staurosporine	ND	0.3 ± 0.02
Tamoxifen	50 ± 0.03	ND

T47-D and 293 cells were cultured in Petri dishes in the presence of different anti-neoplastic drugs: cisplatin (100–400 μM), staurosporine (0.1–400 μM), tamoxifen (12.5–75 μM), or taxol (0.1–0.4 μM). IC_{50} value was determined after 24 h in 293 monolayer cultures, except for taxol (48 h); and after 48 h in T-47D monolayer cultures, except for tamoxifen (24 h). Values represent mean ± SD of five different preparations.

(T-47D) that produce spheroids in almost 1 month were selected. T-47D spheroids of 21 days ($1.2 \pm 0.05\,mm^3$) and 293 spheroids of 8 days ($1.4 \pm 0.05\,mm^3$) (both named mature spheroids) were dispersed using a PBS–EDTA–trypsin mix. The cells were re-seeded in monolayer at 25% confluence on 24-well plates until sub-confluence was reached (it was named "first passage" or S1); one sample was exposed to drug treatment for 24 h and subjected to protein extraction, while a parallel sample was trypsinized and re-seeded in monolayer again for cellular growth for 2 or 3 days until sub-confluence ("second passage" or S2) was reached. Afterwards, the cells were trypsinized and cultured for three more passages (named S3–S5).

PROTEIN EXTRACTION

Briefly, cells isolated from MTS were incubated in RIPA lysis buffer (RadioImmuno Precipitation Assay Buffer: 1% IGEPAL, 0.5% sodium deoxycholate, 0.1% SDS, 100 mM PMSF). To avoid protein degradation a protease inhibitor cocktail (Roche Applied Science, Germany) was added. The samples were then mechanically disrupted using an insulin syringe and centrifuged at 10,000*g* for 30 min. The cellular supernatants were kept at $-20^{\circ}C$ until use.

WESTERN BLOTTING

Cellular protein (40 μg) was electrophoresed on 12% SDS–PAGE and electroblotted on to PVDF membranes. The blots were incubated in TBS–Tween-20 (0.1%) with 5% non-fat dry milk for 1 h at room temperature. Afterwards, each blot was incubated in fresh blocking solution in the presence of the specific primary antibody overnight at 4°C. After 12 h, the blots were washed four times with TBS–T for 15 min and incubated with 1:3,000 (v/v) horseradish peroxidase-conjugated secondary antibodies for 1 h at room temperature. Finally, they were washed with TBS–T four times for 30 min and subjected to a chemiluminescence reaction. Chemiluminescence was detected using ECL plus Western blotting detection reagents (Amersham Biosciences, UK). hILP/XIAP, B-cell lymphoma-3 (Bcl-3), IκBα, IκBε, p65, p50, p52, tubulin, cellular inhibitor of apoptosis-1 (cIAP-1), and XIAP antibodies (dilutions from 1:200 to 1:1,000) were obtained from BD Biosciences (NJ); anti-mouse IgG (H + L) HRP-conjugate, and anti-rabbit IgG (H + L) HRP-conjugate were from Promega (WI). Actin was a generous gift by Dr. R. Herrera (Instituto Politécnico Nacional, Mexico).

IMMUNOHISTOCHEMISTRY

Spheroids were fixed in 4% formalin for 20 min and washed with PBS, carefully sectioned in 4–8 μm slices and placed on paraffin. The samples were then deparaffinated and rehydrated in graded ethanol and finally incubated in sodium citrate buffer according to Arellano-Llamas et al. [2006]. Endogenous peroxidase activity was blocked with 3% (w/v) H_2O_2 for 5 min, and non-specific conjugation was inhibited with 5% BSA. Each sample was incubated at room temperature with the primary antibody (Ki67, hypoxia-inducible factor-1α (HIF-1α), or Bcl-3, each diluted 1:100) for 30 min, then rinsed with fresh PBS and re-incubated with a secondary antibody (Rabbit Polydetector Bio SB, Santa Barbara, CA) for 30 min. The peroxidase substrate was diaminobenzidine (Dako, Denmark). The slides were finally counterstained with Gill's hematoxylin for 8 min.

TUNEL

Paraffin-spheroid layers of 4–8 μm were examined by a terminal deoxynucleotidyl transferase-mediated deoxyuridine triphosphate nick-end labeling (TUNEL) assay to identify apoptotic cells. Apoptosis was identified by detecting cleaved DNA using the in situ ApoTag Kit (Chemicon International, Temecula, CA) according to the manufacturer's instructions. Briefly, slides were treated with proteinase K (20 μg/ml) for 15 min, then incubated with terminal deoxynucleotidyl transferase buffer for 1 h at 37°C, and washed. Incorporated fluorescein-labeled nucleotide was visualized with an Olympus epifluorescence microscope.

NF-κB MODULATION

To manipulate NF-κB activity, plasmids that induce overexpression of inhibitor of kappa B kinase beta (IκBKβ) and IkBS32/S36 were transfected with Lipofectamine 2000 (Invitrogen), selected for 2 weeks with 450 μg G418/ml, cloned, and expanded before spheroid formation. The IκBKβ plasmid was created by sub-cloning the IκBKβ open-reading frame, amplified by PCR, in a pcDNA 3.1 plasmid (Invitrogen). Expression was verified by Western blotting and the plasmid was sequenced to verify identity and absence of mutations. The plasmid with the dominant negative version of IκB (mutated at serine-32 and -36) was a kind gift by Dr. P. Bauerle (University of Munich). At least three independent experiments were performed, each in triplicate.

siRNA CONSTRUCTION AND TRANSFECTION

siRNA for XIAP was generated by sub-cloning specific or transversed sequences of 21 bp (AGGAGATACCGTGCGGTGCTT) and for Bcl-3 (CAACCTACGGCAGACACCG) into the pSIREN vector (Clontech, CA). All clones were sequenced to verify identity. The siRNAs specificity was verified by RT-PCR and Western blotting. T-47D or 293 cells were transfected with 1 μg of the siRNA construct using Lipofectamine 2000 (Invitrogen) for 6 h in serum-free DMEM and further 12–36 h incubation in DMEM with serum. Then, the cells were selected for 2 weeks with 450 μg/ml of G418, cloned, and expanded.

GENE REPORTER ASSAYS

HeLa cells were stably transfected using Lipofectamine 2000 (Invitrogen) with pHTS-Neo-NF-κB vector (Biomyx, CA), which contains five NF-κB enhancer elements upstream of a luciferase open-reading frame. The cells were then grown as MTS for 2 days and lysed with 1× passive lysis buffer (Promega). Parallel MTS were disaggregated and seeded as monolayers for 12 h and lysed with the same buffer. Transfected cells grown as monolayers without previous culture as MTS were used as control. Protein concentration was determined with a DC Protein Assay kit (BioRad, CA). Luciferase activity in equal amounts of protein was measured with a Dual Luciferase Assay Kit (Promega, Madison) according to the manufacturer's instructions, using a Multimode Detector DTX880 (Beckman Coulter, CA). Experiments were performed three times.

STATISTICAL ANALYSES

Data are expressed as mean ± SEM of the indicated number of separate experiments. The experimental and control groups were compared statistically using an unpaired two-tailed Student's *t*-test;

P-values less than 0.05 were considered significant. For other statistical analyses, ANOVA was used.

RESULTS

CHARACTERIZATION OF TUMOR SPHEROIDS FROM SEVERAL CANCER CELL LINES

All tumor cell lines used in the present study were able to generate spheroids and hence the experiments were carried out with MTS from each cell line. However, for conciseness, only selected results were shown in figures, although similar data were attained with the other tumor cell lines.

MTS of HeLa, 293, T-47D, and KB cells showed different proliferation patterns (Fig. 1A). Although all growth curves showed behavior fitting the Gompertz law, each revealed distinctive characteristics [Deakin, 1975; Mueller-Klieser, 1987]. HeLa ($63 \pm 6\,mm^3$), KB ($96 \pm 4\,mm^3$), and 293 ($80 \pm 13\,mm^3$) MTS reached their maximal sizes after 20, 28, and 16 days,

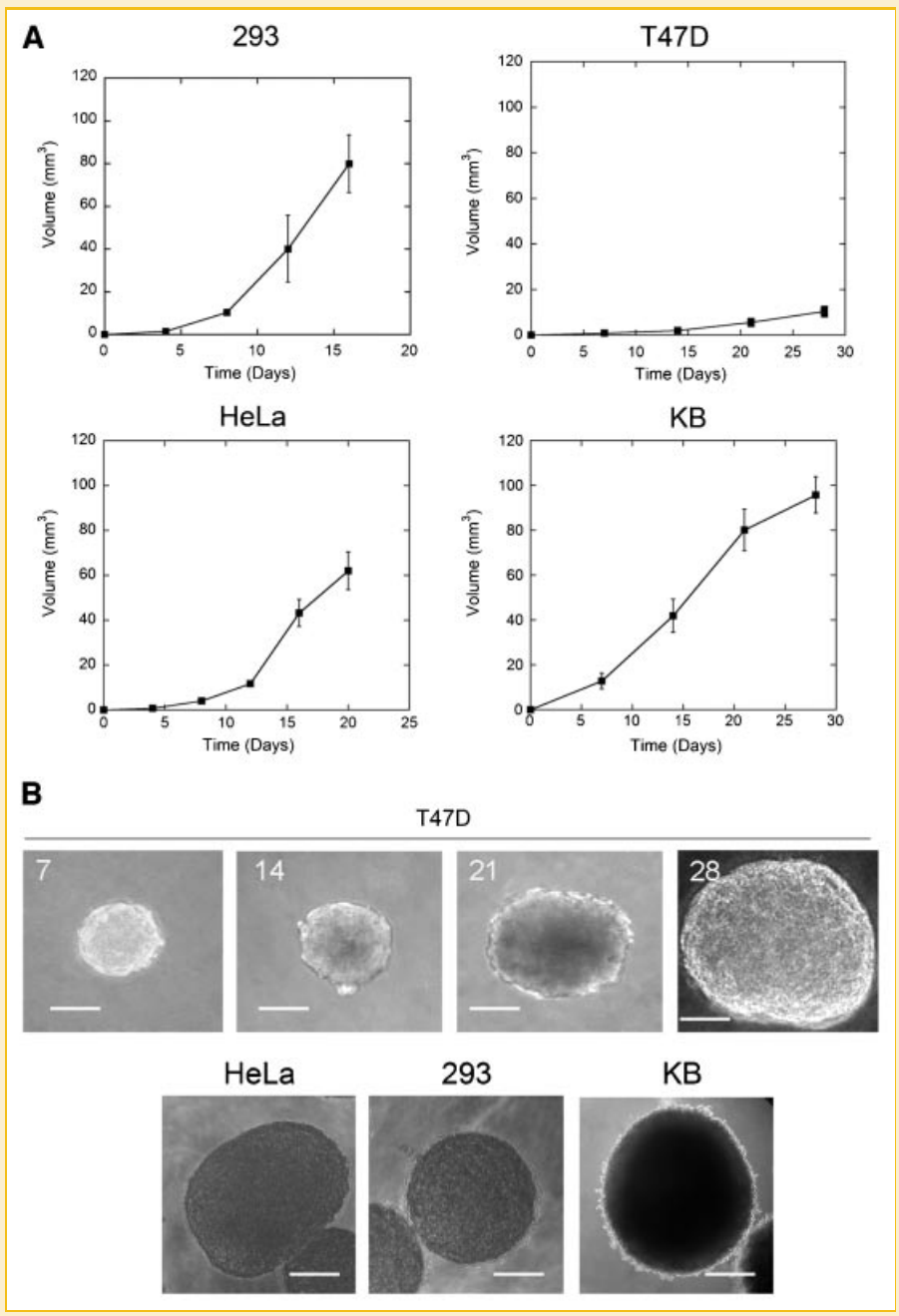

Fig. 1. Growth of multi-cellular tumor spheroids. A: Growth curves of tumor spheroids from 293, T-47D, HeLa, and KB carcinoma cell lines. B: Morphological features of tumor spheroids. Upper panel: Growth of T-47D for the indicated times in days. Lower panel: Mature spheroids derived from HeLa, 293, and KB cancer cells. Bar represents 300 μm. The results are the mean ± SD of four independent experiments.

(diameters of 2, 3.1, and 2.6 mm), respectively. In turn, T-47D MTS showed a lower proliferation rate, forming mature or adult-tumor spheroids ($13.5 \pm 1.8\,mm^3$ and diameter of 0.8 mm) at day 28 ± 2.

It has been pointed out that differences between monolayers versus spheroids are observed when a diameter of 500 μm is reached by MTS [Kunz-Schughart, 1999]. Hence, spheroids of more than 500 μm diameter were used in the following experiments, independently of day of culture.

Structurally, the peripheries of HeLa and KB spheroids were amorphous, suggesting a dispersion of cells at the spheroid's edge. In contrast, MTS from 293 and T-47D cells showed compact structures with well-defined edges (Fig. 1B).

As has been described for human glioma cells, prostate and cervical cancer spheroids, MTS from HeLa, 293, KB, and T-47D developed three characteristic cellular layers [Ng et al., 1986; Gronvik et al., 1996; Sauer et al., 1998]. The intermediate and central cellular layers showed high HIF-1α expression and low levels of Ki67 protein (a cellular proliferation marker) in comparison with the external layer; in addition, a well-defined apoptotic center was detected in all spheroids (Fig. 2).

DRUG RESISTANCE IN TUMOR SPHEROIDS

It is well documented that MTS derived from human ovarian, prostate, and breast cancer are less sensitive to metabolic and anti-neoplastic drugs (2-deoxyglucose, gossypol, vinblastin, doxorubicin) and proteasome inhibitors such as PS-341 than their monolayer counterparts [Frankel et al., 2000; Walker et al., 2004; Rodriguez-Enriquez et al., 2008]. To assess drug resistance in 293, T-47D, HeLa, and KB MTS without interference from different drug diffusion rates, the spheroid cells were gently separated and cultured as monolayers before drug exposure. The proliferation rates of MTS and monolayer cells derived from them were similar, indicating no apparent changes in cell replication (data not shown). As shown by the IC_{50} values (Table I), MTS-derived 293 cells were significantly more resistant to taxol, cisplatin, and staurosporine than their respective original monolayer cultures (Fig. 3A). MTS-derived T-47D cells also showed higher resistance

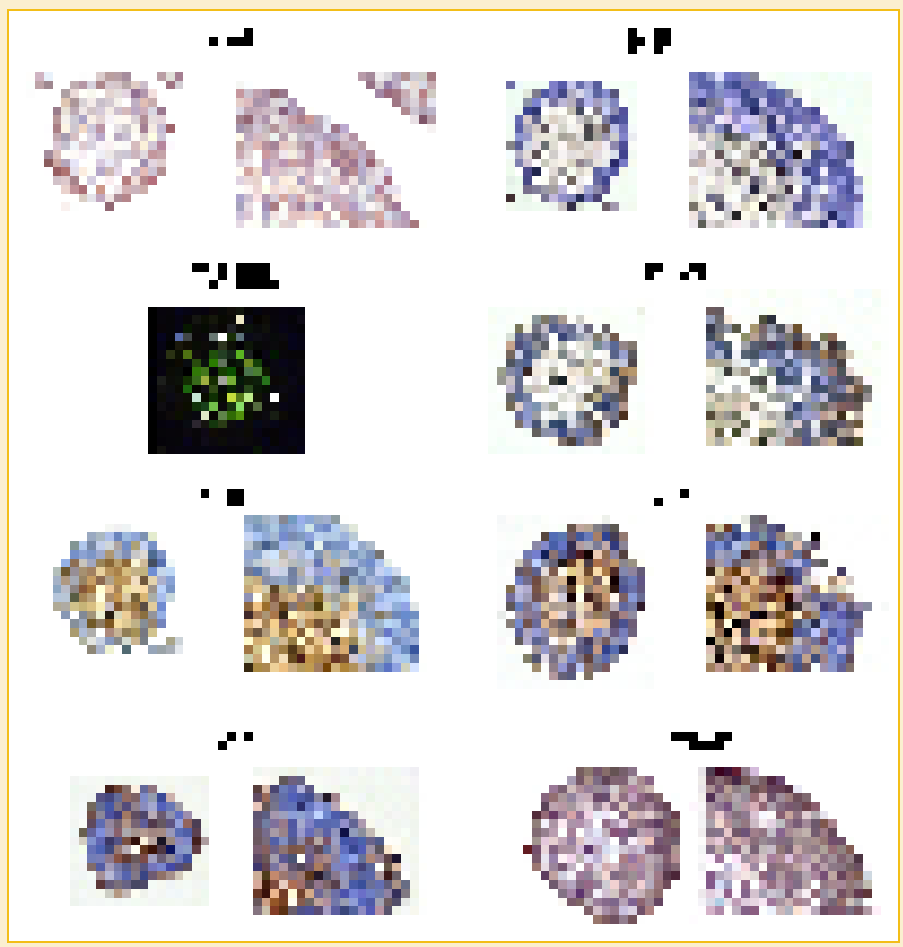

Fig. 2. Characterization of multi-cellular tumor spheroids. Representative inmunohistochemistry of mature T-47D spheroid at 21 days of culture showing signal for Ki67, HIF-1α, Bcl-3, p50, p65, and p52. Magnification 20×, insets 40×. Bar represents 300 μm. In addition, a TUNEL reaction was performed to reveal apoptotic cells.

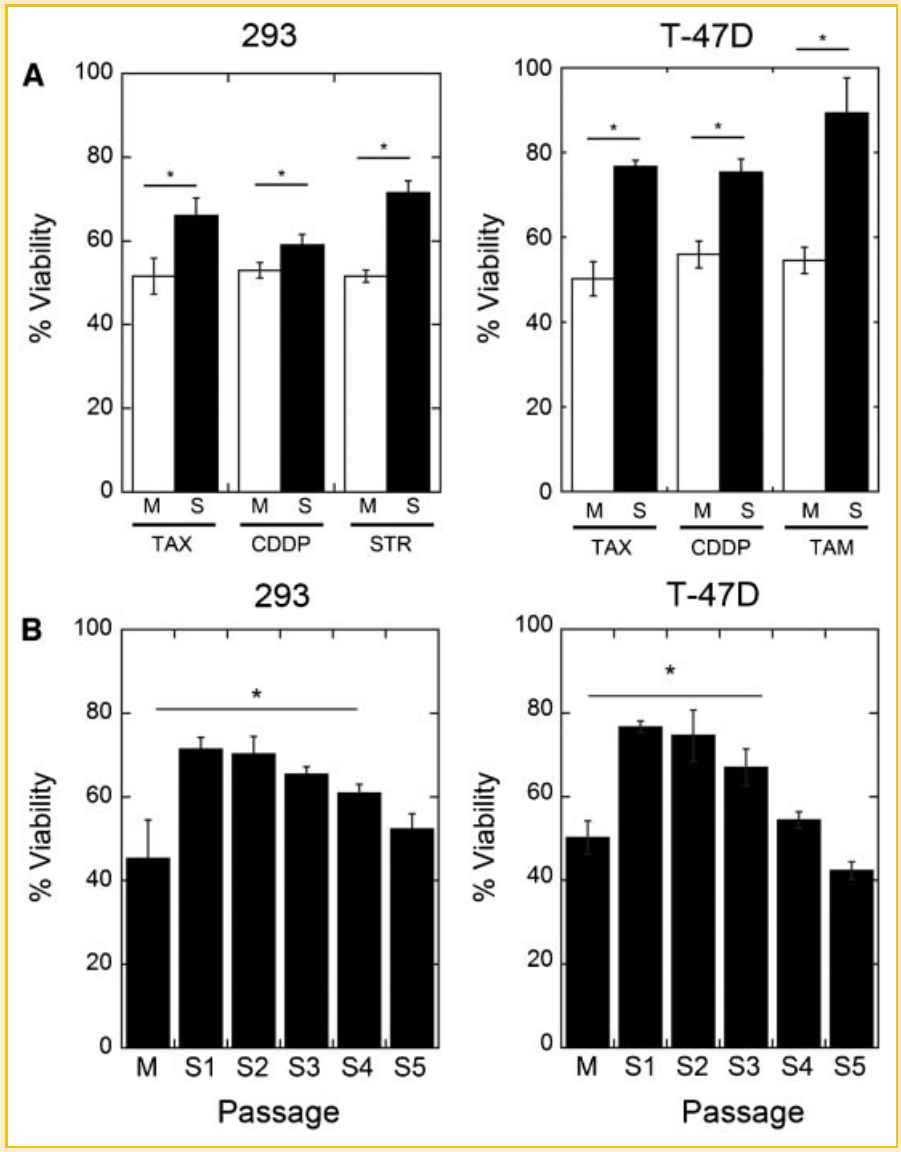

Fig. 3. Growth of tumor cells as multi-cellular tumor spheroids induces resistance to anti-neoplastic agents. A: Mature spheroids of 293 ($70 \pm 2.6\,mm^3$) or T-47D ($13 \pm 0.09\,mm^3$) cells were disaggregated and reseeded for 48 h. The IC_{50} values for taxol (TAX), cisplatin (CDDP), tamoxifen (TAM), and staurosporine (STR) identified in monolayer cultures (Table I) were applied for an additional 24 or 48 h. Left panel: 293 cells, right panel: T-47D cells. Abbreviations: M, monolayer; S, mature spheroids; B: 293 (left panel) or T-47D (right panel) spheroid-derived cells grown as monolayers (S1: first passage; S2: second passage; and so on). Each passage was exposed to IC_{50} values (see Table I) of anti-neoplastic drugs and viability was measured. Results are the mean ± SD of five independent experiments performed in quintuplicate.

to taxol, cisplatin, and tamoxifen (Fig. 3A). However, the spheroids viability data should be interpreted with caution since some cells are dying or dead, and the exposure to trypsin for disaggregation may induce further damage, increasing trypan-blue-positive cells.

Tamoxifen was the drug used at the highest concentration, because the four cell lines employed here were ER (estrogen receptor) negative and tamoxifen targets cells via ER. In consequence, relatively higher concentrations of tamoxifen (with respect to taxol or staurosporine) were required to induce an inhibitory effect. Similar results were obtained for the other two tumor cell lines tested (HeLa and KB, data not shown). The higher drug resistance phenotype was apparent in MTS-derived monolayer cultures after 3–4 passages (12–15 cellular generations) (Fig. 3B).

CHANGES IN THE NF-κB SURVIVAL PATHWAY IN TUMOR SPHEROIDS

It is well established that NF-κB decreases the sensitivity of monolayer tumor cell cultures to diverse anti-cancer drugs through expression of proteins that inhibit apoptosis and cell-cycle progression [Cilloni et al., 2006]. Hence, NF-κB transcriptional activity and protein content were determined in MTS. In agreement with the increased drug resistance, the level of NF-κB was higher in HeLa spheroids of $43 \pm 6\,mm^3$ than in their monolayer counterpart

(Fig. 4A). Proliferation data indicate a higher rate (>30–40%) in HeLa monolayer cells than in spheroids (data not shown). The NF-κB increase was maintained in monolayer cultures derived from these MTS. S/M culture showed a higher NF-κB transcriptional activity than the MTS because the latter included viable and dead cells, whereas S/M cells only included viable cells.

Furthermore, increased expression of IκBα (a regulator of the canonical route and a direct target of NF-κB) and of Bcl-3, an atypical regulator of the non-canonical NF-κB survival pathway, was also detected (Fig. 4B). In contrast, levels of IκBε (a late regulator of p65 and p50) remained unaltered in both cultures. In accordance with the transcriptional activity data (Fig. 4A), the protein levels of the main NF-κB sub-units, p65 and p50 proteins, were also higher in three-dimensional cultures than in monolayer cultures (Fig. 4B). The cellular location of Bcl-3 was mainly nuclear in the cells of the MTS intermediate and hypoxic layers, suggesting that Bcl-3 is transcriptionally active in these regions, as opposed to the external layer, where the location was cytosolic (Fig. 2). Similarly, p50, p52, and p65 were also nuclear in the intermediate and hypoxic layers (Fig. 2). These results showed that the expression of proteins from the NF-κB transduction pathway, and probably its increased activity, was associated with the hypoxic center of the MTS.

XIAP AND CIAP-1 LEVELS IN MTS

The expression levels of other proteins involved in NF-κB-mediated protection against apoptosis, XIAP, and cIAP-1 (two well-characterized apoptosis inhibitor proteins) were analyzed in MTS. Overexpression of IAPs may play a role in tumor cell resistance to drug-induced apoptosis [Notarbartolo et al., 2004]. Both IAPs are directly regulated by NF-κB [Stehlik et al., 1998; Wang et al., 1998; Bandala et al., 2001]. Indeed, cIAP-1 and XIAP protein levels in T-47D and 293 tumor spheroids were 1.5–2.5 times higher than in their monolayer counterparts (Fig. 5A). In situ analyses showed that XIAP is expressed mainly in the intermediate spheroid layers, correlating with the expression of HIF-1, although significant expression was also found in the outer layer (Fig. 2).

Analysis of the time courses of both IAPs in MTS revealed that cIAP-1 levels increased after the initial stages of spheroid formation, whereas the cIAP and XIAP levels were markedly higher at the later spheroid stages (Fig. 5C) and remained constant after the spheroids reached their maximal size ($73.6 \pm 0.6\,mm^3$ for 293 and $9.2 \pm 0.3\,mm^3$ for T-47D). Furthermore, when the spheroids were disaggregated and the cells seeded on Petri dishes, the high IAP levels were maintained until the third passage (Fig. 5B), which correlated with the increased drug resistance phenotype of MTS, that was also maintained in monolayer cultures (Fig. 3B). Similar patterns were also observed for HeLa and KB MTS and S/M cultures (data not shown).

INHIBITION OF NF-κB AND XIAP EXPRESSION MODIFIES THE GROWTH OF MTS AND ITS RESISTANCE AGAINST CHEMOTHERAPY

To further elucidate the role of NF-κB on MTS formation, growth, and increased drug resistance, siRNA technology and negative

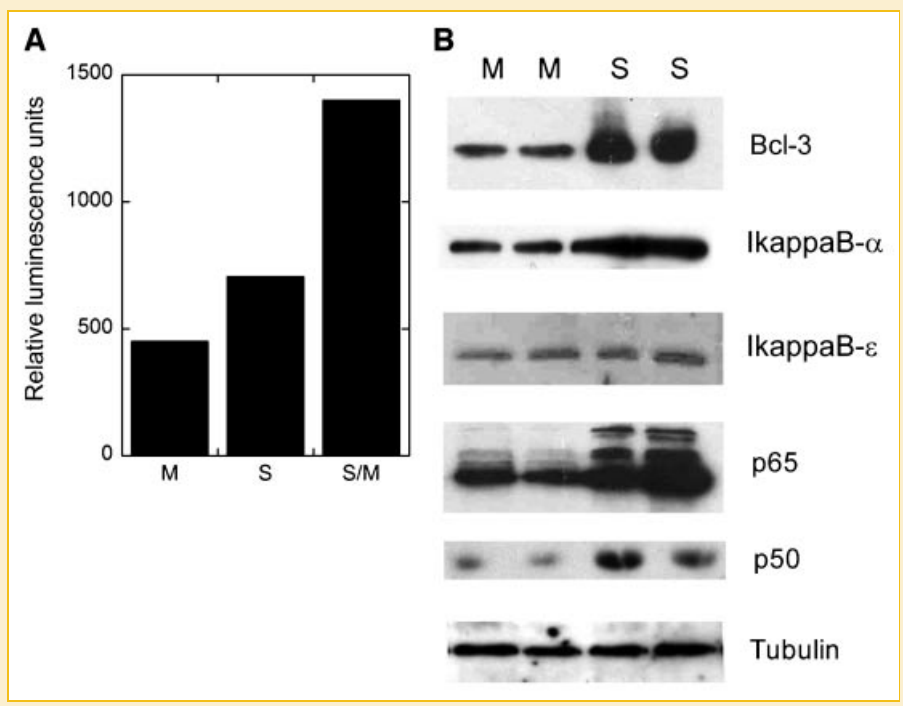

Fig. 4. MTS formation activates NF-κB transduction pathway. A: NF-κB transcriptional activity determined by gene reporter assays. HeLa cells stably transfected with a plasmid containing a luciferase gene under the control of tandem consensus sites for NF-κB were grown (Reporter cell line HeRNFKB) as multi-cellular tumor spheroids or monolayers. They were lysed and equal amounts of protein were assayed for luciferase activity. The panel shows a representative experiment of three independent assays. Abbreviations: M, monolayer culture; S: multi-cellular tumor spheroids; S/M, cells disaggregated from multi-cellular spheroids and grown as monolayers for 12 h. B: Western blot of NF-κB components in monolayer cells and tumor spheroids. Total protein extracts were prepared from mature multi-cellular spheroids and parallel control monolayer cultures. Equal amounts of protein were subjected to SDS–PAGE and immunoblotted with Bcl-3, IκBα, IκB ε, p50, p65, and p52 antibodies. The panel shows two independent experiments of four. Abbreviations: M, monolayer culture; S, multi-cellular tumor spheroids.

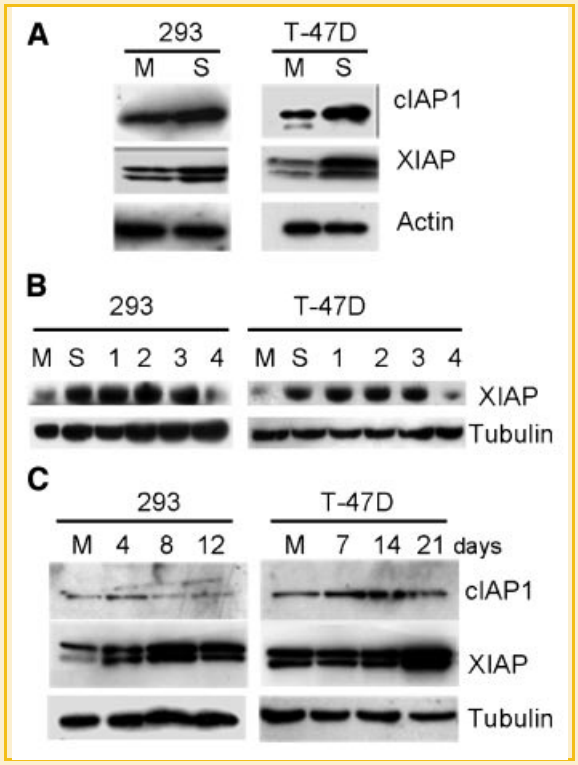

Fig. 5. IAP levels in multi-cellular tumor spheroids. Total protein extracts were prepared from mature multi-cellular spheroids and parallel control monolayer cultures. Equal amounts of protein were subjected to SDS–PAGE and immunoblotted against inhibitor of apoptosis proteins (IAPs). At least three replicates were performed. A: Representative immunoblot of XIAP and cIAP-1 in monolayer versus mature spheroids of 293 and T-47D. B: Representative immunoblot of XIAP in passages 1–5 of disaggregated tumor spheroid cells. C: Representative immunoblot of XIAP and cIAP-1 during 293 or T-47D MTS growth. Experiments were performed four times.

dominants were used to regulate nuclear factor activity and XIAP expression [Devroe and Silver, 2004] (Fig. 6A). The addition of siRNAs to block XIAP production in T-47D and 293 monolayer cultures brought about the formation of smaller spheroids (1.79 ± 0.5 and $2.6 \pm 0.4\,mm^3$, respectively, at days 28 and 16, respectively) in comparison with the wild-type cells (9.2 ± 0.3 and $73.6 \pm 1.4\,mm^3$, respectively) (Fig. 6B), suggesting that activation of the apoptosis machinery precludes spheroid maturity and growth. Cell death by caspase activation was not evaluated here, although other cellular XIAP-mediated processes, such as deregulation of cell cycle (XIAP can activate Akt, a signal protein that induces cell-cycle progression) might also affect spheroid growth [Yamaguchi et al., 1999]. This remains to be evaluated. Interestingly, the smaller T-47D and 293 spheroids were 35–45% more sensitive to taxol and staurosporine than normal spheroids (Fig. 6C). HeLa and KB monolayer cells treated with siRNA XIAP and cultured as MTS showed a similar altered behavior (data not shown).

On the other hand, inhibition of the NF-κB pathway, with an IκBε-expressing dominant or by using Bcl-3-siRNA, promoted a drastic reduction (80%) in the size of the spheroids formed (from 26.5 ± 6.4 to $4.4 \pm 0.1\,mm^3$ at day 16 ± 2), which prevented reliable analysis of drug resistance in these MTS (Fig. 7A). Overexpression of IκBKβ (the main upstream NF-κB activator) induced a significant fourfold increase in the size of HeLa MTS (from 45 ± 5 to $195 \pm 21\,mm^3$) (Fig. 7B), suggesting that NF-κB is essential for spheroid formation and growth.

DISCUSSION

Several authors have described a close similarity between three-dimensional tumor cell models and solid small avascular tumors [MacDonald and Howell, 1978; MacDonald et al., 1978; Lord and Nardella, 1980; Mueller-Klieser, 1997; Kunz-Schughart, 1999]. Indeed, MTS formed from T-47D, 293, HeLa, and KB cells showed the classic three-dimensional geometry comprising two specific cellular layers and an apoptotic center. Growth of MTS from T-47D, 293, HeLa, and KB cells followed Gompertz-type kinetics, although each particular cell line developed a distinctive proliferation rate and maximal size. In the outer cellular layer of the MTS there was specific overexpression of certain genes such as Ki67 protein, indicating active cellular proliferation; in contrast, overexpression of HIF-1α was found mainly in the intermediate cellular layer, reflecting a lower oxygen concentration.

NF-κB-deficient HeLa cells in monolayer culture maintained high viability and proliferation rates (data not shown), indicating that NF-κB has a negligible role in the control of cell-cycle progression, at least in these cells. In contrast, during MTS development the inner cell layers undergo hypoxic stress, which may lead to apoptosis and growth delay; however, NF-κB-deficient cells did not form mature spheroids, but only small cellular aggregates ($4.4 \pm 0.1\,mm^3$), suggesting that NF-κB was essential for the assembly, formation, and maturity of tumor multi-cellular spheroids. The well-known anti-apoptotic effect of NF-κB on the viability of non-tumorigenic cells might be involved [Egan et al., 2004]. However, other processes may also take place to support apoptotic events in three-dimensional models [Barbone et al., 2008].

Regarding the specific mechanisms of NF-κB up-regulation, it has been documented that a hypoxic environment and low pH, similar to that found in the spheroid center, activates NF-κB [Cummins et al., 2007]. Supporting our data, a previous report has shown that NF-κB is activated in glioma spheroids, becoming relatively resistant to TNF-α [Sudheerkumar et al., 2008]. Although not studied, IAPs could mediate this resistance, since it is well known that they can also repress apoptosis induced by TNF-α [Uren et al., 1996]. It is noteworthy that XIAP, which is regulated by NF-κB, was found in the intermediate layer of the three-dimensional structures, where HIF-1α was also expressed (Fig. 2), supporting the view that hypoxia and low pH have a role in NF-κB activation. In this regard, it has shown that NF-κB trans-activates the HIF-1α gene and induces the accumulation of its protein, and this is an important physiological contributor to the hypoxic response [Rius et al., 2008].

Cells derived from MTS and further cultured in 24-well plates showed increased resistance to cisplatin, taxol, staurosporine, and tamoxifen (Fig. 3A). Interestingly, MTS-derived cells preserved the higher drug resistance phenotype for several generations, indicating a stable change in the genetic and biochemical regulatory

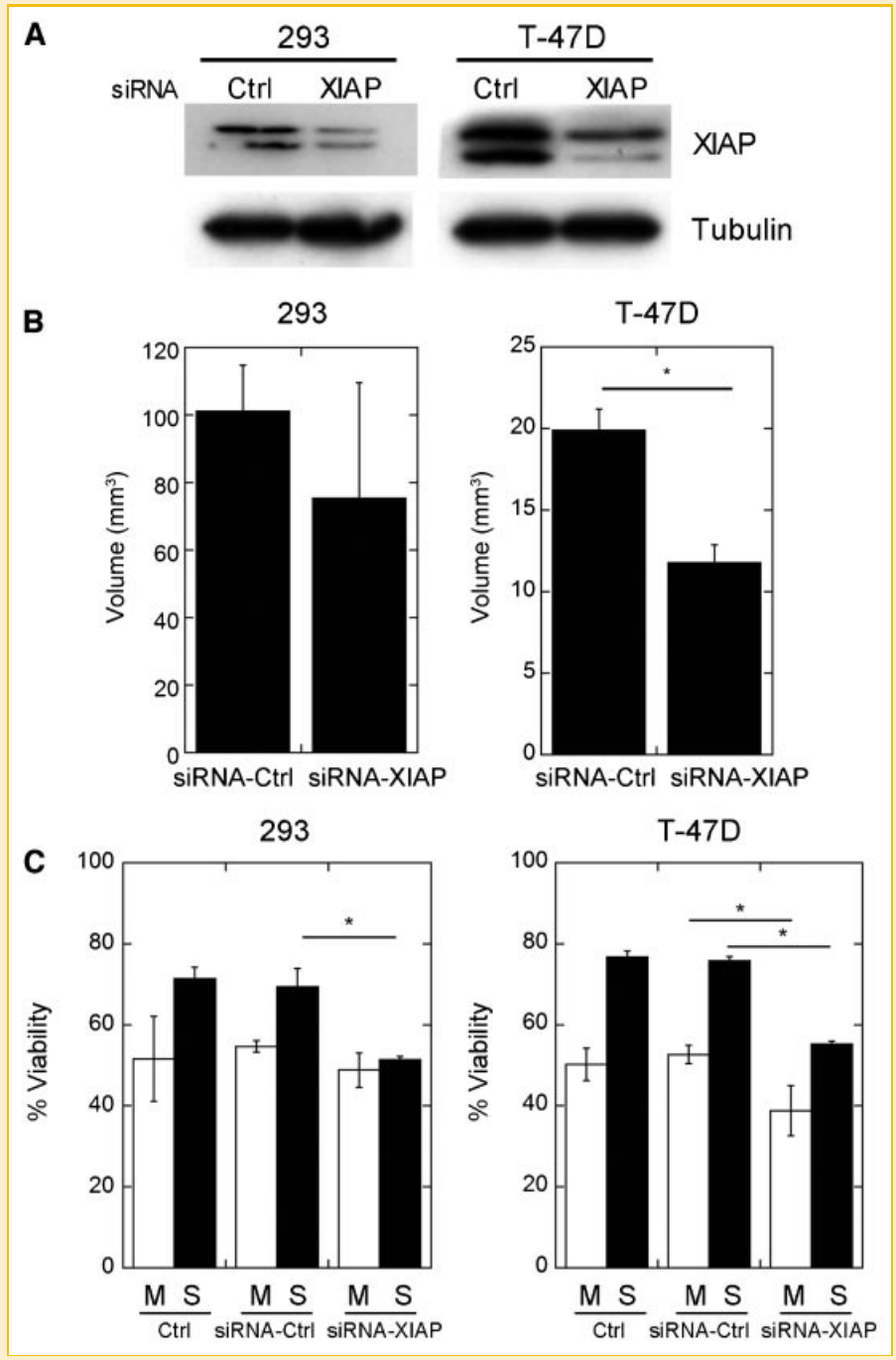

Fig. 6. Effect of XIAP siRNA on MTS growth and anti-neoplastic resistance. 293 and T-47D MTS were stably transfected with a XIAP siRNA-expressing vector. A: XIAP down-regulation visualized by Western blotting. B: 293 and T-47D cells with stable XIAP silencing were used to generate MTS; their volumes were compared with those derived from cells expressing a control siRNA. C: 293 and T-47D cells with silenced XIAP or expressing a control siRNA were used to generate MTS. After reaching maturity, these MTS were disaggregated, cultured for an additional 48 h, and exposed to IC_{50} values of staurosporine for 293 and taxol for T47-D (Table I) for a further 24 h; viability was measured by staining with crystal violet. Results are the mean ± SD of three independent experiments performed in triplicate. Abbreviations: M, monolayer culture; S, cells derived from multi-cellular tumor spheroids.

mechanisms. This phenomenon correlated with the persistent activation of NF-κB in these cells.

Another stable change was the elevated IAP content. In this regard, it is known that hypoxia activates IκBKβ, the main upstream modulator of NF-κB, providing a possible mechanism for the activation of this transcription factor [Cummins et al., 2006]. This change could be perpetuated by a positive feedback mediated by cytokine production, since cells cultured in MTS show a cytokine auto-regulatory loop mediated by a stress response [Jack et al., 2007]. Further experiments inhibiting these loops could help to

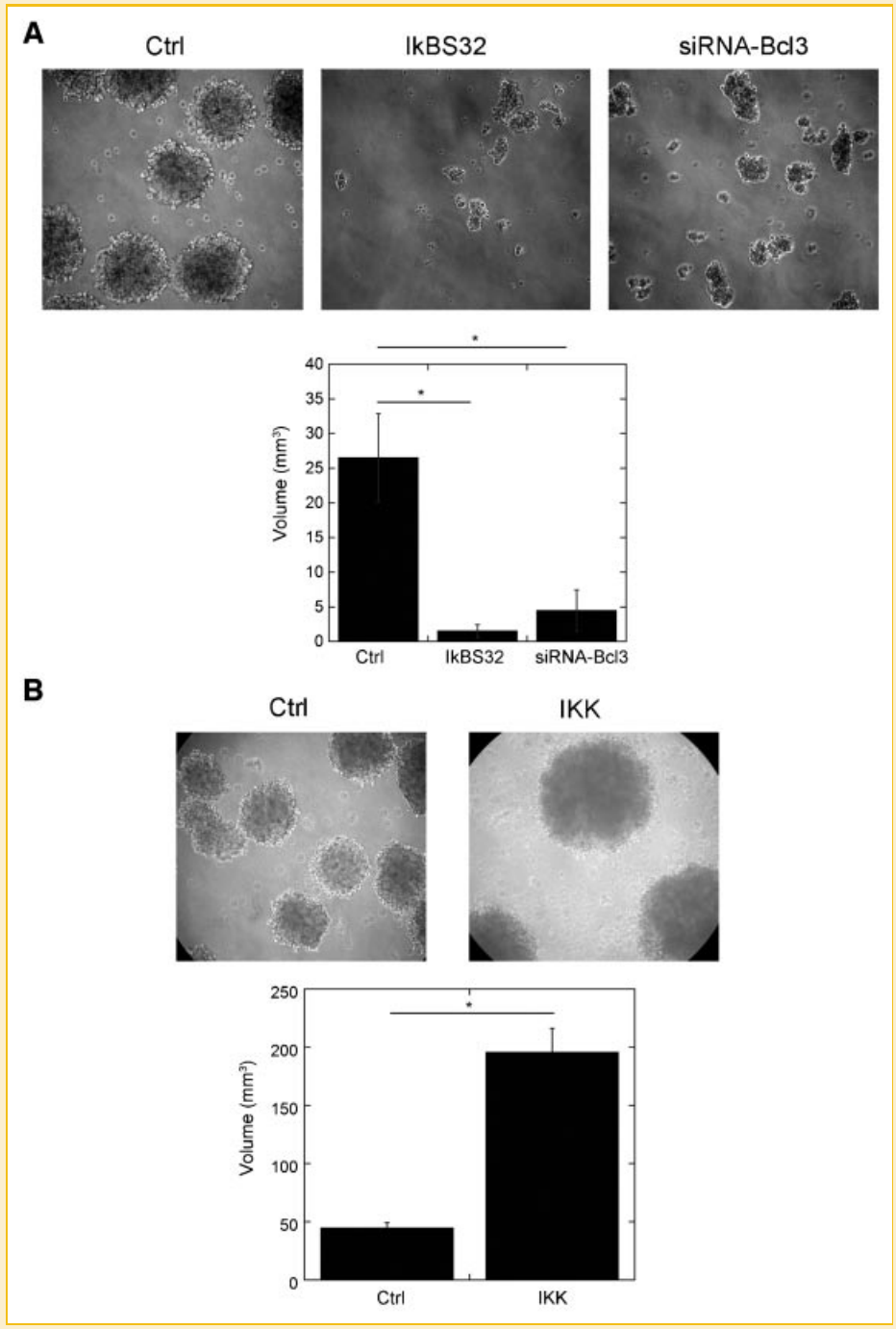

Fig. 7. NF-κB pathway regulates MTS growth. The NF-κB pathway was suppressed or activated by the transfection of plasmids that express either a dominant-negative version of the IκBα inhibitor, a siRNA directed to Bcl-3, or the upstream activator of the pathway, IκBKβ. A: Inhibition of the NF-κB pathway. Micrographs showing the morphology (upper panel) and volume (lower panel) of spheroids derived from cells expressing the dominant-negative version of IκBα, IkBS32, or an siRNA directed toward Bcl-3. B: Activation of the NF-κ B pathway. Micrographs showing the morphology (upper panel) and volume (lower panel) of spheroids derived from cells that overexpress the NF-κB pathway activator IκBKβ (IKK). Results are the mean ± SD of three independent experiments performed in triplicate.

answer this question. Also, an epigenetic mechanism might be involved in the increased drug resistance of MTS.

Both XIAP and cIAP-1 levels remained elevated in spheroid-derived monolayer cultures, and this correlated with the acquired drug resistance phenotype. The decrease in XIAP levels induced by RNAi transfection brought about a significant diminution in spheroid growth (65%), which was lower than that achieved by NF-κB blocking. These findings suggested that NF-κB modulates other genes associated with the cell-cycle regulation or cell survival pathways [Karin, 2006]. In turn, both IAP repression and NF-κB blocking led to a return of the drug-dependent apoptosis threshold in cellular spheroids to values similar to those found in original

monolayers. Therefore, the data from the present study indicated that the increase of XIAP mediated by NF-κB plays an important role in the increased drug resistance of MTS.

A clinically relevant problem in cancer treatment is the ability of tumor cells to develop drug resistance. However, most studies on this subject have been carried out on tumor cell monolayer cultures. In the monolayer culture model, cells are exposed to a homogeneous environment regarding oxygen concentration, nutrients, pH, and growth factors. This feature does not resemble the physiological microenvironment inside of a solid tumor that favors drug resistance. In consequence, a model that better mimics the presence of a microenvironment with oxygen and other metabolite gradients should be used for studies on drug resistance. Interestingly, we found that in tumor spheroids NF-κB could be a pharmacological target, because its inhibition blocked tumor growth in vitro. As tumor spheroids represent the first stages of tumor growth (before vascularization), the findings of the present study suggested that tumor growth can be inhibited and sensitized to chemotherapy more effectively in earlier stages of formation by targeting NF-κB.

ACKNOWLEDGMENTS

This work was supported by grant CONACYT CO1 42309 from the Consejo Nacional de Ciencia y Tecnologia, México, to V. Maldonado. J.C. Gallardo-Pérez was supported by a fellowship from CONACYT and the present work was part of his doctoral thesis from the UNAM in Biomedical Sciences Doctorate Program, Faculty of Medicine.

REFERENCES

Arellano-Llamas A, Garcia FJ, Perez D, Cantu D, Espinosa M, De la Garza JG, Maldonado V, Melendez-Zajgla J. 2006. High Smac/DIABLO expression is associated with early local recurrence of cervical cancer. BMC Cancer 6:256.

Baker FL, Spitzer G, Ajani JA, Brock WA, Lukeman J, Pathak S, Tomasovic B, Thielvoldt D, Williams M, Vines C, Tofilon P. 1986. Drug and radiation sensitivity measurements of successful primary monolayer culturing of human tumor cells using cell-adhesive matrix and supplemented medium. Cancer Res 46:1263–1274.

Bandala E, Espinosa M, Maldonado V, Melendez-Zajgla J. 2001. Inhibitor of apoptosis-1 (IAP-1) expression and apoptosis in non-small-cell lung cancer cells exposed to gemcitabine. Biochem Pharmacol 62:13–19.

Barbone D, Yang TM, Morgan JR, Gaudino G, Broaddus VC. 2008. Mammalian target of rapamycin contributes to the acquired apoptotic resistance of human mesothelioma multicellular spheroids. J Biol Chem 283:13021–13030.

Bonello S, Zahringer C, BelAiba RS, Djordjevic T, Hess J, Michiels C, Kietzmann T, Gorlach A. 2007. Reactive oxygen species activate the HIF-1alpha promoter via a functional NFkappaB site. Arterioscler Thromb Vasc Biol 27:755–761.

Burkowski FJ. 1977. A computer simulation of the growth of a tumour in vitro. Comput Programs Biomed 7:203–210.

Cilloni D, Messa F, Arruga F, Defilippi I, Morotti A, Messa E, Carturan S, Giugliano E, Pautasso M, Bracco E, Rosso V, Sen A, Martinelli G, Baccarani M, Saglio G. 2006. The NF-kappaB pathway blockade by the IKK inhibitor PS1145 can overcome imatinib resistance. Leukemia 20:61–67.

Cummins EP, Berra E, Comerford KM, Ginouves A, Fitzgerald KT, Seeballuck F, Godson C, Nielsen JE, Moynagh P, Pouyssegur J, Taylor CT. 2006. Prolyl hydroxylase-1 negatively regulates IkappaB kinase-beta, giving insight into hypoxia-induced NFkappaB activity. Proc Natl Acad Sci USA 103:18154–18159.

Cummins EP, Comerford KM, Scholz C, Bruning U, Taylor CT. 2007. Hypoxic regulation of NF-kappaB signaling. Methods Enzymol 435:479–492.

Deakin AS. 1975. Model for the growth of a solid in vitro tumor. Growth 39:159–165.

Dertinger H, Hulser D. 1981. Increased radioresistance of cells in cultured multicell spheroids. I. Dependence on cellular interaction. Radiat Environ Biophys 19:101–107.

Devroe E, Silver PA. 2004. Therapeutic potential of retroviral RNAi vectors. Expert Opin Biol Ther 4:319–327.

Egan LJ, Eckmann L, Greten FR, Chae S, Li ZW, Myhre GM, Robine S, Karin M, Kagnoff MF. 2004. IkappaB-kinasebeta-dependent NF-kappaB activation provides radioprotection to the intestinal epithelium. Proc Natl Acad Sci USA 101:2452–2457.

Frankel A, Man S, Elliott P, Adams J, Kerbel RS. 2000. Lack of multicellular drug resistance observed in human ovarian and prostate carcinoma treated with the proteasome inhibitor PS-341. Clin Cancer Res 6:3719–3728.

Freyer JP. 1998. Decreased mitochondrial function in quiescent cells isolated from multicellular tumor spheroids. J Cell Physiol 176:138–149.

Gronvik C, Capala J, Carlsson J. 1996. The non-variation in radiosensitivity of different proliferative states of human glioma cells. Anticancer Res 16:25–31.

Jack GD, Cabrera MC, Manning ML, Slaughter SM, Potts M, Helm RF. 2007. Activated stress response pathways within multicellular aggregates utilize an autocrine component. Cell Signal 19:772–781.

Kang HG, Jenabi JM, Zhang J, Keshelava N, Shimada H, May WA, Ng T, Reynolds CP, Triche TJ, Sorensen PH. 2007. E-cadherin cell-cell adhesion in ewing tumor cells mediates suppression of anoikis through activation of the ErbB4 tyrosine kinase. Cancer Res 67:3094–3105.

Karin M. 2006. Nuclear factor-kappaB in cancer development and progression. Nature 441:431–436.

Khaitan D, Chandna S, Arya MB, Dwarakanath BS. 2006. Establishment and characterization of multicellular spheroids from a human glioma cell line; Implications for tumor therapy. J Transl Med 4:12.

Kolchinsky A, Roninson IB. 1997. Drug resistance conferred by MDR1 expression in spheroids formed by glioblastoma cell lines. Anticancer Res 17:3321–3327.

Kunz-Schughart LA. 1999. Multicellular tumor spheroids: Intermediates between monolayer culture and in vivo tumor. Cell Biol Int 23:157–161.

Lord EM, Nardella G. 1980. The multicellular tumor spheroid model. II. Characterization of the primary allograft response in unsensitized mice. Transplantation 29:119–124.

MacDonald HR, Howell RL. 1978. The multicellular spheroid as a model tumor allograft. I. Quantitative assessment of spheroid destruction in alloimmune mice. Transplantation 25:136–140.

MacDonald HR, Howell RL, McFarlane DL. 1978. The multicellular spheroid as a model tumor allograft. II. Characterization of spheroid-infiltrating cytotoxic cells. Transplantation 25:141–145.

Mekhail TM, Markman M. 2002. Paclitaxel in cancer therapy. Expert Opin Pharmacother 3:755–766.

Mueller-Klieser W. 1987. Multicellular spheroids. A review on cellular aggregates in cancer research. J Cancer Res Clin Oncol 113:101–122.

Mueller-Klieser W. 1997. Three-dimensional cell cultures: From molecular mechanisms to clinical applications. Am J Physiol 273:C1109–C1123.

Nachmias B, Ashhab Y, Ben-Yehuda D. 2004. The inhibitor of apoptosis protein family (IAPs): An emerging therapeutic target in cancer. Semin Cancer Biol 14:231–243.

Ng CE, Keng PC, Sutherland RM. 1986. Density distributions of human squamous carcinoma cells: Influence of growth conditions, proliferative status and DNA content. Int J Cancer 38:413–418.

Notarbartolo M, Cervello M, Giannitrapani L, Meli M, Poma P, Dusonchet L, Montalto G, D'Alessandro N. 2004. Expression of IAPs and alternative splice variants in hepatocellular carcinoma tissues and cells. Ann N Y Acad Sci 1028:289–293.

Okamoto T, Sanda T, Asamitsu K. 2007. NF-kappa B signaling and carcinogenesis. Curr Pharm Des 13:447–462.

Olive PL, Durand RE. 1994. Drug and radiation resistance in spheroids: Cell contact and kinetics. Cancer Metastasis Rev 13:121–138.

Oloumi A, MacPhail SH, Johnston PJ, Banath JP, Olive PL. 2000. Changes in subcellular distribution of topoisomerase IIalpha correlate with etoposide resistance in multicell spheroids and xenograft tumors. Cancer Res 60:5747–5753.

Philchenkov A. 2004. Caspases: Potential targets for regulating cell death. J Cell Mol Med 8:432–444.

Piva R, Belardo G, Santoro MG. 2006. NF-kappaB: A stress-regulated switch for cell survival. Antioxid Redox Signal 8:478–486.

Rius J, Guma M, Schachtrup C, Akassoglou K, Zinkernagel AS, Nizet V, Johnson RS, Haddad GG, Karin M. 2008. NF-kappaB links innate immunity to the hypoxic response through transcriptional regulation of HIF-1alpha. Nature 453: 807–811.

Rodriguez-Enriquez S, Gallardo-Perez JC, Aviles-Salas A, Marin-Hernandez A, Carreno-Fuentes L, Maldonado-Lagunas V, Moreno-Sanchez R. 2008. Energy metabolism transition in multi-cellular human tumor spheroids. J Cell Physiol 216:189–197.

Sauer H, Ritgen J, Hescheler J, Wartenberg M. 1998. Hypotonic Ca2+ signaling and volume regulation in proliferating and quiescent cells from multicellular spheroids. J Cell Physiol 175:129–140.

Shweiki D, Neeman M, Itin A, Keshet E. 1995. Induction of vascular endothelial growth factor expression by hypoxia and by glucose deficiency in multicell spheroids: Implications for tumor angiogenesis. Proc Natl Acad Sci USA 92:768–772.

St Croix B, Florenes VA, Rak JW, Flanagan M, Bhattacharya N, Slingerland JM, Kerbel RS. 1996. Impact of the cyclin-dependent kinase inhibitor p27Kip1 on resistance of tumor cells to anticancer agents. Nat Med 2: 1204–1210.

Stehlik C, de Martin R, Kumabashiri I, Schmid JA, Binder BR, Lipp J. 1998. Nuclear factor (NF)-kappaB-regulated X-chromosome-linked iap gene expression protects endothelial cells from tumor necrosis factor alpha-induced apoptosis. J Exp Med 188:211–216.

Sudheerkumar P, Shiras A, Das G, Jagtap JC, Prasad V, Shastry P. 2008. Independent activation of Akt and NF-kappaB pathways and their role in resistance to TNF-alpha mediated cytotoxicity in gliomas. Mol Carcinog 47:126–136.

Sutherland RM. 1988. Cell and environment interactions in tumor microregions: The multicell spheroid model. Science 240:177–184.

Uren AG, Pakusch M, Hawkins CJ, Puls KL, Vaux DL. 1996. Cloning and expression of apoptosis inhibitory protein homologs that function to inhibit apoptosis and/or bind tumor necrosis factor receptor-associated factors. Proc Natl Acad Sci USA 93:4974–4978.

Walker J, Martin C, Callaghan R. 2004. Inhibition of P-glycoprotein function by XR9576 in a solid tumour model can restore anticancer drug efficacy. Eur J Cancer 40:594–605.

Wang CY, Mayo MW, Korneluk RG, Goeddel DV, Baldwin AS, Jr. 1998. NF-kappaB antiapoptosis: Induction of TRAF1 and TRAF2 and c-IAP1 and c-IAP2 to suppress caspase-8 activation. Science 281:1680–1683.

Xing H, Wang S, Weng D, Chen G, Yang X, Zhou J, Xu G, Lu Y, Ma D. 2007. Knock-down of P-glycoprotein reverses taxol resistance in ovarian cancer multicellular spheroids. Oncol Rep 17:117–122.

Yamaguchi K, Nagai S, Ninomiya-Tsuji J, Nishita M, Tamai K, Irie K, Ueno N, Nishida E, Shibuya H, Matsumoto K. 1999. XIAP, a cellular member of the inhibitor of apoptosis protein family, links the receptors to TAB1-TAK1 in the BMP signaling pathway. EMBO J 18:179–187.

Yuhas JM, Li AP, Martinez AO, Ladman AJ. 1977. A simplified method for production and growth of multicellular tumor spheroids. Cancer Res 37:3639–3643.

Zhivotovsky B, Orrenius S. 2006. Carcinogenesis and apoptosis: Paradigms and paradoxes. Carcinogenesis 27:1939–1945.